

Using frequency detuning to improve the sensitivity of electric field measurements via electromagnetically induced transparency and Autler-Townes splitting in Rydberg atoms

Matt T. Simons, Joshua A. Gordon, Christopher L. Holloway, David A. Anderson, Stephanie A. Miller, and Georg Raithel

Citation: [Applied Physics Letters](#) **108**, 174101 (2016); doi: 10.1063/1.4947231

View online: <http://dx.doi.org/10.1063/1.4947231>

View Table of Contents: <http://scitation.aip.org/content/aip/journal/apl/108/17?ver=pdfcov>

Published by the [AIP Publishing](#)

Articles you may be interested in

[Millimeter wave detection via Autler-Townes splitting in rubidium Rydberg atoms](#)

Appl. Phys. Lett. **105**, 024104 (2014); 10.1063/1.4890094

[Sub-wavelength imaging and field mapping via electromagnetically induced transparency and Autler-Townes splitting in Rydberg atoms](#)

Appl. Phys. Lett. **104**, 244102 (2014); 10.1063/1.4883635

[Electromagnetically induced transparency and fluorescence in blockaded Rydberg atomic system](#)


J. Chem. Phys. **139**, 164316 (2013); 10.1063/1.4826637

[New Possibilities for Electric Field Measurements in a Plasma with the Use of Laser and Stark Spectroscopy](#)





AIP Conf. Proc. **645**, 413 (2002); 10.1063/1.1525482

[Measurements of Local Electric Fields in Low Density Plasmas via Stark-Splitting of Hydrogen Resonance Lines](#)

AIP Conf. Proc. **645**, 86 (2002); 10.1063/1.1525440



Instruments for Advanced Science

<p>Contact Hiden Analytical for further details: www.HidenAnalytical.com info@hiden.co.uk</p> <p>CLICK TO VIEW our product catalogue</p>	 <p>Gas Analysis</p> <ul style="list-style-type: none"> » dynamic measurement of reaction gas streams » catalysis and thermal analysis » molecular beam studies » dissolved species probes » fermentation, environmental and ecological studies 	 <p>Surface Science</p> <ul style="list-style-type: none"> » UHV TPD » SIMS » end point detection in ion beam etch » elemental mapping - surface mapping 	 <p>Plasma Diagnostics</p> <ul style="list-style-type: none"> » plasma source characterization » etch and deposition process reaction » kinetic studies » analysis of neutral and radical species 	 <p>Vacuum Analysis</p> <ul style="list-style-type: none"> » partial pressure measurement and control of process gases » reactive sputter process control » vacuum diagnostics » vacuum coating process monitoring
----------------------------------------------------------------------------------------------------------------------------------------------------------------------------------------------------------------------------------------------	----------------------------------------------------------------------------------------------------------------------------------------------------------------------------------------------------------------------------------------------------------------------------------------------------------------------------------------------------------------------------------------------	----------------------------------------------------------------------------------------------------------------------------------------------------------------------------------------------------------------------------------------------------------------------------------------------	----------------------------------------------------------------------------------------------------------------------------------------------------------------------------------------------------------------------------------------------------------------------------------------------------------------------------------------	----------------------------------------------------------------------------------------------------------------------------------------------------------------------------------------------------------------------------------------------------------------------------------------------------------------------------------------------------------

Using frequency detuning to improve the sensitivity of electric field measurements via electromagnetically induced transparency and Autler-Townes splitting in Rydberg atoms

Matt T. Simons,¹ Joshua A. Gordon,¹ Christopher L. Holloway,^{1,a)} David A. Anderson,^{2,b)} Stephanie A. Miller,² and Georg Raithel²

¹National Institute of Standards and Technology (NIST), Boulder, Colorado 80305, USA

²Department of Physics, University of Michigan, Ann Arbor, Michigan 48109, USA

(Received 3 March 2016; accepted 31 March 2016; published online 26 April 2016)

In this work, we demonstrate an approach for improved sensitivity in weak radio frequency (RF) electric-field strength measurements using Rydberg electromagnetically induced transparency (EIT) in an atomic vapor. This is accomplished by varying the RF frequency around a resonant atomic transition and extrapolating the weak on-resonant field strength from the resulting off-resonant Autler-Townes (AT) splittings. This measurement remains directly traceable to SI compared to previous techniques, precluding any knowledge of experimental parameters such as optical beam powers as is the case when using the curvature of the EIT line shape to measure weak fields. We use this approach to measure weak RF fields at 182 GHz and 208 GHz demonstrating improvement greater than a factor of 2 in the measurement sensitivity compared to on-resonant AT splitting RF electric field measurements. [<http://dx.doi.org/10.1063/1.4947231>]

In a recent work, we (and others) have demonstrated a fundamentally new approach for electric (E) field measurements^{1–5} that can lead to a self-calibrated measurement and has the capability to perform measurements on a fine spatial resolution. The approach utilizes the concept of electromagnetically induced transparency (EIT).^{1,2,6} Consider a sample of stationary four-level atoms illuminated by a single weak (“probe”) light field, as depicted in Fig. 1. In this approach, one laser is used to probe the response of the atoms and a second laser is used to excite the atoms to a Rydberg state (the coupling laser). In the presence of the coupling laser, the atoms become transparent to the probe laser transmission (this is the concept of EIT). The coupling laser wavelength is chosen such that the atom is at a high enough state such that an radio frequency (RF) field can cause an atomic transition of the atom. The RF transition in this four-level atomic system causes a splitting of the transmission spectrum (the EIT signal) for a probe laser. This splitting of the probe laser spectrum is easily measured and is directly proportional to the applied RF E-field amplitude (through Planck’s constant and the dipole moment of the atom), see Ref. 1 for details of the technique’s theory. By measuring this splitting (Δf_m), we get a direct measurement of the magnitude of the RF E-field strength for a time-harmonic field from the following:¹

$$|E| = 2\pi \frac{\hbar \lambda_p}{\wp \lambda_c} \Delta f_m = 2\pi \frac{\hbar}{\wp} \Delta f_o, \quad (1)$$

where λ_p and λ_c are the wavelengths of the probe and coupling lasers, Δf_m is the measured splitting and $\Delta f_o = \frac{\lambda_p}{\lambda_c} \Delta f_m$, \hbar is the Planck’s constant, and \wp is the atomic dipole moment of the RF transition (see Ref. 1 for discussion on determining \wp and values for various atomic states). The ratio $\frac{\lambda_p}{\lambda_c}$ accounts for the Doppler mismatch of the counter propagating probe and

coupling lasers,⁶ resulting from the different wavelengths interacting with the moving atoms. We consider this type of measurement of the E-field strength a direct, SI-traceable, self-calibrated measurement in which it is related to the Planck’s constant (which will become an SI quantity defined by standard bodies in the near future) and only requires a frequency measurement (Δf_m , which can be measured very accurately).

This technique has shown promise to measure moderate to high field strengths.^{1,7–9} However, it can pose some difficulties for weak field strength, which can be a problem when performing the measurements for frequencies in the upper millimeter-wave and sub-THz bands where power levels can be low. For weak field strength, it can be difficult to detect and measure the splitting in the EIT signal. The problem of measuring Δf_m for these high frequencies is made worse because of the size of the dipole moment (\wp) of the RF driven Rydberg-Rydberg transition. The measurement at these high frequencies requires a small principal atomic number (n), or a low Rydberg state, and the values of the dipole moments (\wp) for these low n are significantly smaller than those for the lower GHz range (or large n range), see Fig. 6 in Ref. 1. Thus, since the measured Δf_m is directly proportional to the product of “ $\wp |E|$ ” (see Refs. 1 and 2), when the E-field strength is weak and the frequencies are high (small n , and in turn, small values of \wp), the ability to measure Δf_m becomes problematic. In this paper, we demonstrate an approach to mitigate this.

A typical measured EIT signal for this technique is shown in Fig. 2 for the cases with and without RF applied. The experimental setup for these measurements is shown in Fig. 1. We use a cylindrical glass vapor cell of length 75 mm and diameter 25 mm containing rubidium-85 (⁸⁵Rb) atoms. The levels $|1\rangle$, $|2\rangle$, $|3\rangle$, and $|4\rangle$ correspond, respectively, to the ⁸⁵Rb $5S_{1/2}$ ground state, $5P_{3/2}$ excited state, and two Rydberg states. The probe is a 780 nm laser which is scanned across the $5S_{1/2}$ – $5P_{3/2}$ transition. The probe beam is focused

^{a)}Electronic mail: holloway@boulder.nist.gov

^{b)}Also at Rydberg Technologies, Ann Arbor, Michigan 48104.

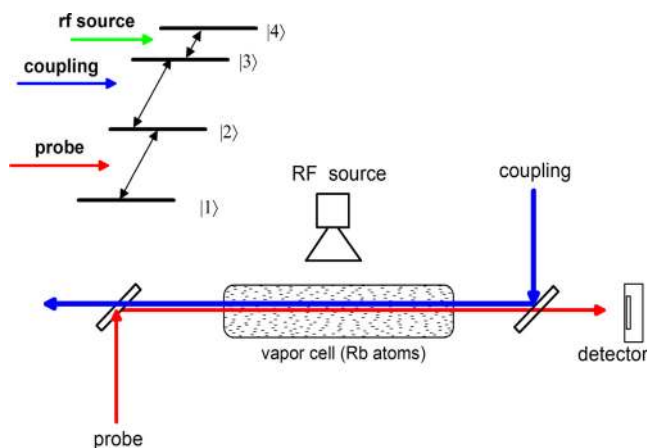


FIG. 1. Illustration of a four-level system, and the vapor cell setup for measuring EIT, with counter-propagating probe and coupling beams. The RF is applied transverse to the optical beam propagation in the vapor cell.

to a full-width at half maximum (FWHM) of $94\ \mu\text{m}$, with a power of $17.5\ \mu\text{W}$. To produce an EIT signal, we apply a counter-propagating coupling laser (wavelength $\lambda_c \approx 480\ \text{nm}$) with a power of $32\ \text{mW}$, focused to an FWHM of $144\ \mu\text{m}$. The coupling laser is tuned near the $5P_{3/2}$ – $26D_{5/2}$ Rydberg transition ($\lambda_c = 483.924\ \text{nm}$). We modulate the coupling laser amplitude with a $30\ \text{kHz}$ square wave and detect any resulting modulation of the probe transmission with a lock-in amplifier. This removes the Doppler background and isolates the EIT signal, as shown in the solid curve of Fig. 2. The application of RF (via a horn antenna placed $265\ \text{mm}$ from the vapor cell) at $132.646\ \text{GHz}$ to couple states $26D_{5/2}$ and $27P_{3/2}$ splits the EIT peak as shown by the dashed curve in the figure. We measure the frequency splitting of the EIT peaks in the probe spectrum, Δf_m , and determine the E-field amplitude using (1) as shown in Fig. 2.

The power levels stated in the figure caption (and stated throughout the paper) are the power reading of the signal generator (SG) that feeds the waveguide which, in turn, feeds the horn antenna. Due to the losses in the feeding waveguide, the reflections and losses in the horn antenna, and propagation losses, this is not the power level (or E-field strength) incident onto the vapor cell.

The difficulties of measuring a splitting for weak field strength are shown in Fig. 3. These data were collected with the same experimental parameters as the data shown in Fig. 2 except for a low SG RF power (or $-44\ \text{dBm}$) or low incident E-field strength. Here, we see that it is difficult to distinguish a splitting in the EIT signal.

We should add that the ability to distinguish the splitting in the EIT line is a function of the width of the EIT signal. This line width is a function of various parameters ranging from laser line width, to Doppler broadening, to power of both the probe and coupling lasers. Several of these effects are discussed in Ref. 10. In this paper, we will discuss an approach to improve minimum detectable splitting for a “given” EIT line width, and not discuss how to minimize the EIT line width.

We can overcome this difficulty of measuring a small Δf_m by using an RF detuning method. When an RF field is detuned from its resonant transition frequency, it has two main effects on the observed splitting of the EIT signal.

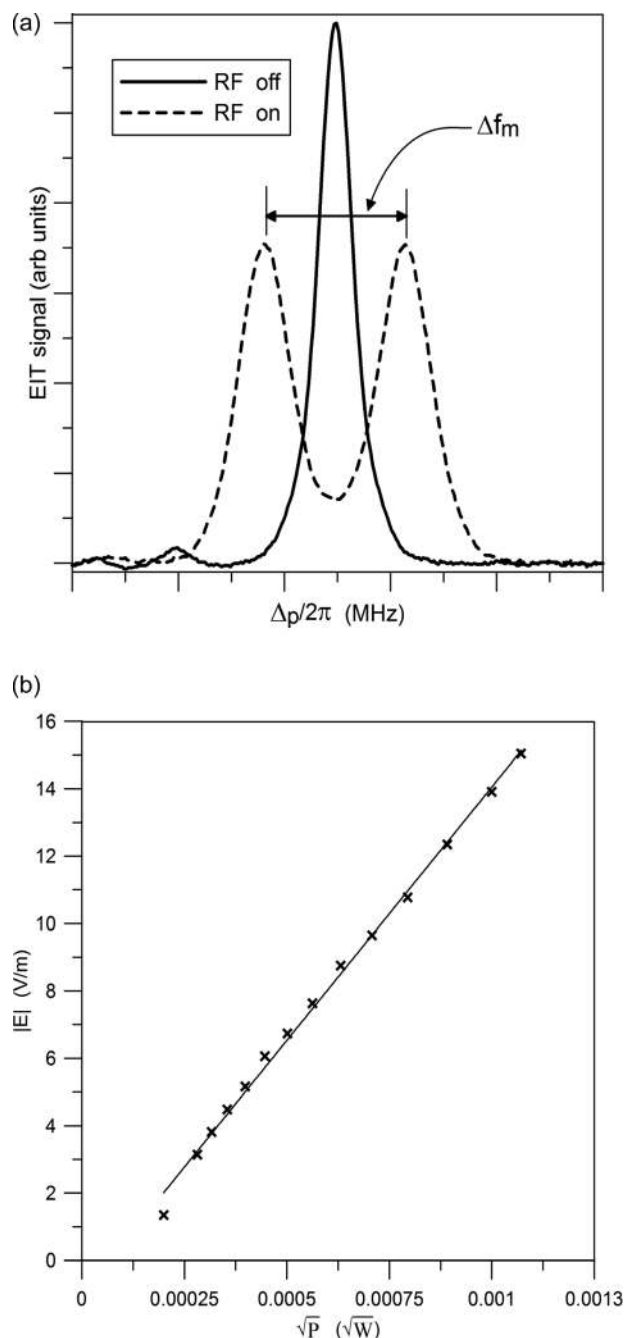
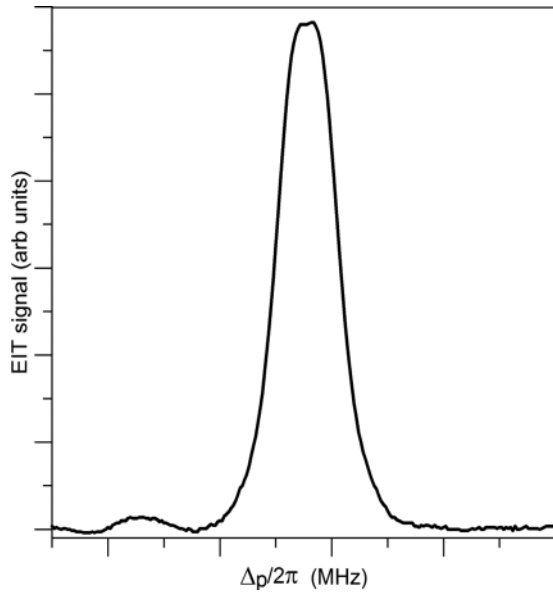


FIG. 2. This dataset is for $132.6459\ \text{GHz}$ and corresponds to this following 4-level atomic system: $5S_{1/2} - 5P_{3/2} - 26D_{5/2} - 27P_{3/2}$. (a) Illustration of the EIT signal (i.e., probe laser transmission through the cell) as a function of probe laser detuning Δp . The SG RF power level is $-29.4\ \text{dBm}$. (b) Estimated E-field.

First, the two peaks of the EIT signal are non-symmetric (i.e., the heights of the two peaks are not the same). Figure 4 shows two examples where the RF is detuned $\pm 50\ \text{MHz}$ and $\pm 30\ \text{MHz}$ on either side of the resonant transition frequency for a $26D_{5/2} - 27P_{3/2}$ transition (Fig. 4(a) is for an SG power level of $-29.4\ \text{dBm}$ and Fig. 4(b) is for $-44.0\ \text{dBm}$). The on-resonant RF frequency for this transition is $133.6459\ \text{GHz}$. We see from the figure that if the RF frequency is lower than the on-resonant frequency, the left peak is lower than the right. If the RF frequency is higher than the on-resonant frequency, the right peak is lower than the left. The second effect of the RF detuning is that the separation

FIG. 3. EIT signal for 132.6459 GHz and RF power of -44 dBm.

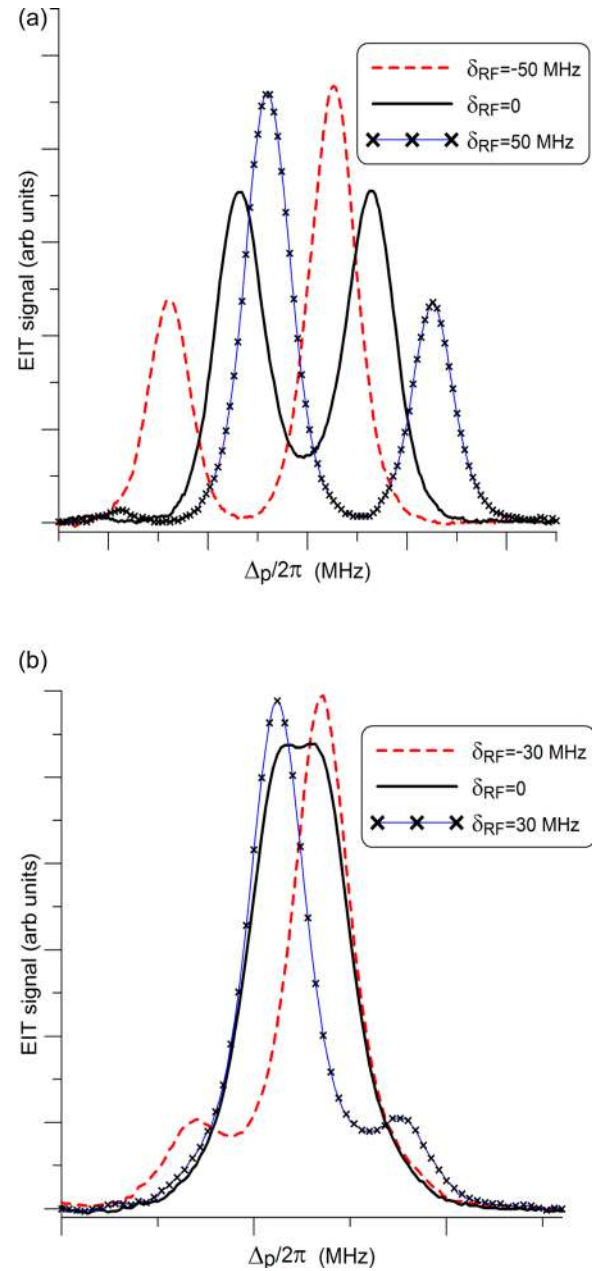
between the two peaks increases with RF detuning. The peak separation (measured in MHz) with the RF detuning is given by the following:¹¹

$$\Delta f_{\delta} = \sqrt{(\delta_{RF})^2 + (\Delta f_o)^2}, \quad (2)$$

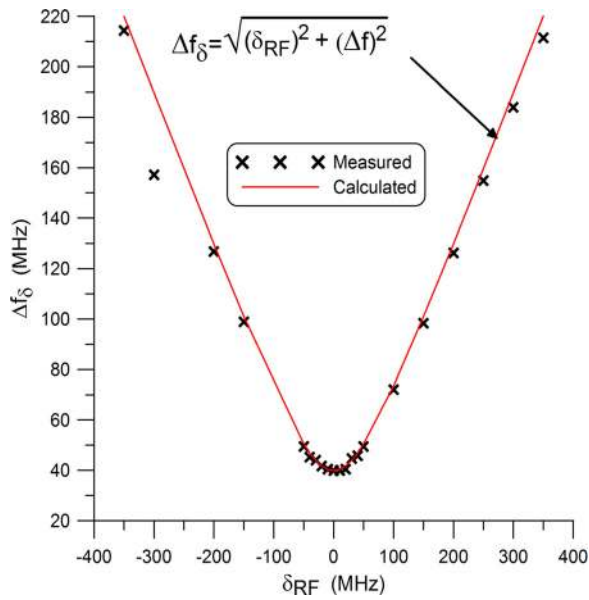
where δ_{RF} is the RF detuning ($\delta_{RF} = f_o - f_{RF}$; f_o is the on-resonance RF transition and f_{RF} the frequency of the RF source) and Δf_o is the separation of the two peaks with no RF detuning (or when $\delta_{RF} = 0$). Figure 5 shows the experimental data for Δf_{δ} for $26D_{5/3} - 27P_{3/2}$. Notice that the experimental data agree well with Equation (2).

By performing a series of measurements for various RF detunings, a data set can be fit to the above expression in order to determine Δf_o for weak RF fields, which in turn can be used in Eq. (1) to calculate $|E|$. To illustrate this, we performed two sets of RF detuning experiments at 208.30 GHz (to couple states $23D_{5/2}$ and $22F_{7/2}$) and 182.149 GHz (to couple states $24D_{5/2}$ and $23F_{7/2}$). These results are shown in Fig. 6. In this figure, we show data for various SG power levels. In these experiments, the probe is a 780 nm laser which is scanned across the $5S_{1/2} - 5P_{3/2}$ transition and focused to an FWHM of $75 \mu\text{m}$, with a power of $30 \mu\text{W}$. To produce an EIT signal, we apply a counter-propagating coupling laser (wavelength $\lambda_c \approx 480 \text{ nm}$) with a power of 53 mW , focused on an FWHM of $140 \mu\text{m}$. For the 208.30 GHz measurement, we tuned the coupling laser near the $5P_{3/2} - 23D$ Rydberg transition or $\lambda_c = 484.49 \text{ nm}$, and for the 182.149 GHz measurement, we tuned the coupling laser near the $5P_{3/2} - 24D$ Rydberg transition or $\lambda_c = 484.02 \text{ nm}$. A horn antenna placed at 47 mm (197 mm for 182.15 GHz) from the vapor cell is used for the RF source.

For the 208.3 GHz measurements, the four SG power levels were low enough that the E-field strength at the vapor cell was too small to see any splitting in the EIT signal for $\delta_{RF} = 0$. For all four of the SG power levels, the EIT signals are similar to those shown in Fig. 3, in which it was difficult

FIG. 4. EIT signal for (a) SG power level of -29.4 dBm and $\delta_{RF} = \pm 50$ MHz and (b) SG power level of -44.0 dBm and $\delta_{RF} = \pm 30$ MHz.

to distinguish any Autler-Townes (AT) splitting. This is indicated in Fig. 6 by noting that there are no data for $\delta_{RF} = 0$ and data can only be collected for $|\delta_{RF}| \geq 5 \text{ MHz}$. That is, no splitting could be observed in the EIT signal unless the RF was detuned by 5 MHz ; hence, the E-field strength could not be determined. However, by fitting the data to the expression given in (2), Δf_o can be estimated. The data sets for the four different SG power levels were fit to the expression in Eq. (2). These fits were used to determine Δf_o and values are given in Table I. Also in the table are the calculated E-fields at the vapor cell obtained from Eq. (1). The dipole moment for this transition was calculated to be $\varphi = 317.141 e a_o$ (which includes an angular part of 0.4899 since co-linear RF and optical beams were used). The blank entries in the table for the splitting measurements (i.e., no RF detuning) indicate that AT splitting could not be observed and no data could be

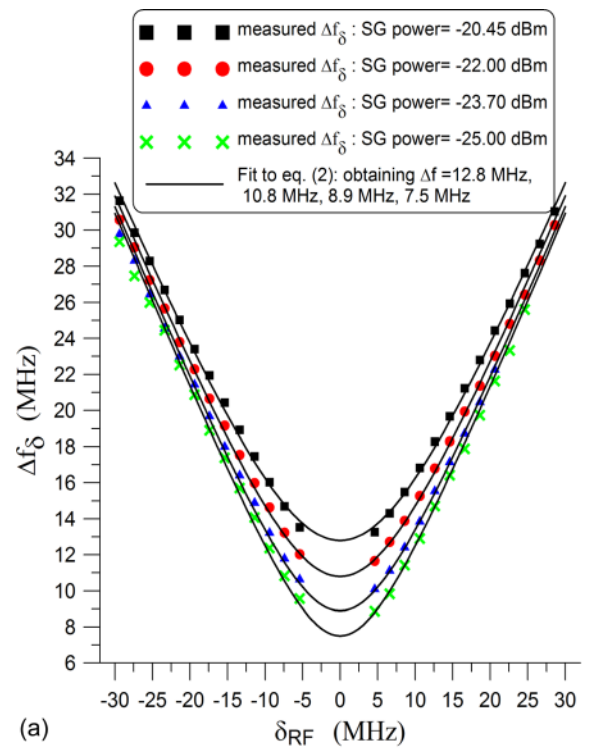
FIG. 5. Experimental data for Δf_δ for $26D_{5/3}-27P_{3/2}$ for -29.4 dBm.

collected. The results in Fig. 6 and in Table I indicate that with RF detuning it was possible to detect an E-field strength, which was not possible without detuning.

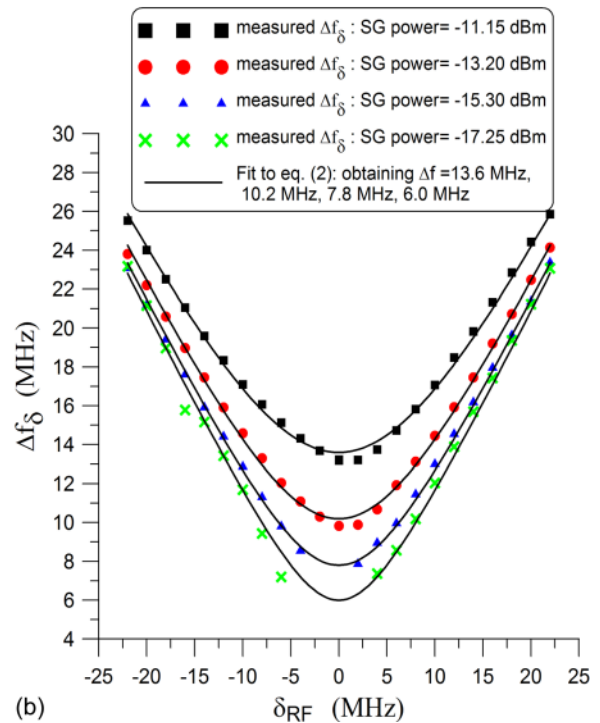
For the 182.149 GHz measurements, we see that for two of the SG power levels, and we do have data for $\delta_{RF} = 0$. However, at some point the SG power levels are low enough that the E-field strength at the vapor cell is too low to detect any splitting for $\delta_{RF} = 0$. This is indicated in Fig. 6 by noting that there are no measured data for $\delta_{RF} = 0$ for SG power equal to -15.30 dBm and -17.25 dBm. However, we do have data for all power levels when $\delta_{RF} \geq 5$ MHz. By fitting the data to the expression given in (2), Δf_o can be determined and the E-field strength for all four SG power levels can be calculated. These values are given in Table I. The table also shows results for the estimated Δf_o and $|E|$ from just measuring the splitting at $\delta_{RF} = 0$. Once again, by using RF detuning we are able to estimate Δf_o and $|E|$ for weak field strength, which is not possible by using just the EIT signal at $\delta_{RF} = 0$ (the blank entries in the table). The dipole moment for this transition was calculated to be $\varphi = 346.529ea_o$ (which includes an angular part of 0.4899 since co-linear RF and optical beams were used). We see that by using the RF detuning approach, we were able to measure an E-field strength of about a factor of 2 smaller than that when the detuning approach is not used. The uncertainties of these types of measurements are currently being investigated.^{1,12,13}

Note that there is a limit for which the detuning approach can still be used. This is explained by referring to Fig. 6. Notice that the wings of the detuning curves approach one another and begin to merge together. When this occurs, the fitting algorithm has difficulty fitting the different datasets to Eq. (2), and in turn has difficulty determining unique values for Δf_o for very-weak E-field strengths.

On a side note, fitting the expression given in Eq. (2) to the RF detuning data also allows us to determine the on-resonant RF transitions (i.e., f_o). This measured f_o allows for us to make comparisons to the calculated values of f_o as determined from quantum defects; in effect, assessing the values of the current



(a)



(b)

FIG. 6. RF detuning experiments: (a) 208.30 GHz and (b) 182.15 GHz.

available quantum defects. A paper detailing this is presently being written. With that said, we fitted Eq. (2) to all the data sets given in Fig. 6 and determined $f_o = 208.305$ GHz for the data in Fig. 6(a) and $f_o = 182.154$ GHz for the data in Fig. 6(b). Using the best available quantum defects for Rb,^{14,15} we calculated these RF transitions to be $f_o = 208.299$ GHz and $f_o = 182.149$ GHz, respectively.

TABLE I. Detuning estimates of Δf_o for 182 GHz and 208 GHz.

208.30 GHz: $23D_{5/2} - 22F_{7/2}$		
SG power level	RF detuning fits to Eq. (2)	On-resonant AT splitting
−20.45 dBm	$\Delta f_o = 12.8$ MHz $ E = 5.08$ V/m	$\Delta f_o = \text{—}$ $ E = \text{—}$
−22.00 dBm	$\Delta f_o = 10.8$ MHz $ E = 4.29$ V/m	$\Delta f_o = \text{—}$ $ E = \text{—}$
−23.75 dBm	$\Delta f_o = 8.9$ MHz $ E = 3.53$ V/m	$\Delta f_o = \text{—}$ $ E = \text{—}$
−25.00 dBm	$\Delta f_o = 7.5$ MHz $ E = 2.98$ V/m	$\Delta f_o = \text{—}$ $ E = \text{—}$
182.15 GHz: $24D_{5/2} - 23F_{7/2}$		
SG power level	RF detuning fits to Eq. (2)	On-resonant AT splitting
−11.15 dBm	$\Delta f_o = 13.6$ MHz $ E = 4.94$ V/m	$\Delta f_o = 13.3$ MHz $ E = 4.84$ V/m
−13.20 dBm	$\Delta f_o = 10.2$ MHz $ E = 3.71$ V/m	$\Delta f_o = 9.83$ MHz $ E = 3.57$ V/m
−15.30 dBm	$\Delta f_o = 7.8$ MHz $ E = 2.84$ V/m	$\Delta f_o = \text{—}$ $ E = \text{—}$
−17.25 dBm	$\Delta f_o = 6.0$ MHz $ E = 2.18$ V/m	$\Delta f_o = \text{—}$ $ E = \text{—}$

In this paper, we have demonstrated a technique based on using frequency detuning to improve the sensitivity of RF E-field measurements via EIT in Rydberg atoms in vapor cells. We presented data for two frequencies that show by using the RF detuning we are able to determine the splitting and E-field strength for weak field levels, which is not possible by using just the EIT signal at $\delta_{RF} = 0$ (i.e., on-resonant AT splitting). The technique presented overcomes the problem with standard EIT measurement approach (i.e., difficulties in detecting and measuring on-resonant splitting in the EIT signal), which can be of particular importance for meas-

urements in upper millimeter-wave and sub-THz bands, where the power levels can be low.

This work was partially supported by the Defense Advanced Research Projects Agency (DARPA) under the QuASAR Program and by NIST through the Embedded Standards program.

- ¹C. L. Holloway, J. A. Gordon, A. Schwarzkopf, D. A. Anderson, S. A. Miller, N. Thaicharoen, and G. Raithel, *IEEE Trans. Antennas Propag.* **62**(12), 6169–6182 (2014).
- ²J. A. Sedlacek, A. Schwettmann, H. Kbler, R. Low, T. Pfau, and J. P. Shaffer, *Nat. Phys.* **8**, 819 (2012).
- ³C. L. Holloway, J. A. Gordon, A. Schwarzkopf, D. A. Anderson, S. A. Miller, N. Thaicharoen, and G. Raithel, *Appl. Phys. Lett.* **104**, 244102 (2014).
- ⁴J. A. Gordon, C. L. Holloway, A. Schwarzkopf, D. A. Anderson, S. A. Miller, N. Thaicharoen, and G. Raithel, *Appl. Phys. Lett.* **105**, 024104 (2014).
- ⁵J. A. Sedlacek, A. Schwettmann, H. Kbler, and J. P. Shaffer, *Phys. Rev. Lett.* **111**, 063001 (2013).
- ⁶A. K. Mohapatra, T. R. Jackson, and C. S. Adams, *Phys. Rev. Lett.* **98**, 113003 (2007).
- ⁷D. A. Anderson, S. A. Miller, A. Schwarzkopf, C. L. Holloway, J. A. Gordon, N. Thaicharoen, and G. Raithel, *Phys. Rev. A* **90**, 043419 (2014).
- ⁸D. A. Anderson, S. A. Miller, G. Raithel, J. A. Gordon, M. L. Butler, and C. L. Holloway, *Phys. Rev. Applied* **5**, 034003 (2016).
- ⁹S. A. Miller, D. A. Anderson, and G. Raithel, e-print [arXiv:1601.06840](https://arxiv.org/abs/1601.06840).
- ¹⁰G. T. Purves, “Absorption and dispersion in atomic vapours: Applications to interferometry,” Ph.D. thesis, Durham University, 2006, Chap. 3.
- ¹¹P. R. Berman and V. S. Malinovsky, *Principles of Laser Spectroscopy and Quantum Optics* (Princeton University Press, 2011).
- ¹²C. L. Holloway, J. A. Gordon, M. T. Simons, H. Fan, S. Kumar, J. P. Shaffer, D. A. Anderson, A. Schwarzkopf, S. A. Miller, N. Thaicharoen, and G. Raithel, “Atom-based RF electric field measurements: An initial investigation of the measurement uncertainties,” in *EMC 2015: Joint IEEE International Symposium on Electromagnetic Compatibility and EMC Europe, Dresden, Germany, August 16–22* (IEEE, 2015), pp. 467–472.
- ¹³H. Fan, S. Kumar, J. Sheng, J. P. Shaffer, C. L. Holloway, and J. A. Gordon, *Phys. Rev. Appl.* **4**, 044015 (2015).
- ¹⁴W. Li, I. Mourachko, M. W. Noel, and T. F. Gallagher, *Phys. Rev. A* **67**, 052502 (2003).
- ¹⁵M. Mack, F. Karlewski, H. Hattermann, S. Höckh, F. Jessen, D. Cano, and J. Fortágh, *Phys. Rev. A* **83**, 052515 (2011).